IEEE Access
Multidisciplinary ⋮ Rapid Review ⋮ Open Access Journal

Received June 19, 2020, accepted July 8, 2020, date of publication July 13, 2020, date of current version July 23, 2020.

Digital Object Identifier 10.1109/ACCESS.2020.3008945

Cost-Effective Printed Electrodes Based on Emerging Materials Applied to Biosignal Acquisition

VÍCTOR TORAL[1], ENCARNACIÓN CASTILLO[1], ANDREAS ALBRETCH[2], FRANCISCO J. ROMERO[1], ANTONIO GARCÍA[1], (Senior Member, IEEE), NOEL RODRÍGUEZ[1], PAOLO LUGLI[3], (Fellow, IEEE), DIEGO P. MORALES[1], AND ALMUDENA RIVADENEYRA[1]

[1]Department of Electronics and Computer Technology, University of Granada, 18071 Granada, Spain
[2]Institute of Nanoelectronics, Technical University of Munich, 80333 Munich, Germany
[3]Faculty of Science and Technology, Free University of Bozen-Bolzano, 39100 Bolzano, Italy

Corresponding author: Víctor Toral (vtoral@ugr.es)

This work was supported in part by the Spanish Ministry of Education, Culture and Sport (MECD)/FEDER-EU through the Project and Predoctoral Grants under Grant TEC2017-89955-P, Grant FPU16/01451, and Grant FPU18/01376, in part by the BBVA Foundation through the 2019 Leonardo Grant for Researchers and Cultural Creators, and in part by the University of Granada through its Projects for Junior Researchers.

ABSTRACT In this paper flexible printed electrodes applicable to wearable electronics are presented. Using innovative materials as Laser Induced Graphene (LIG) and printed electronics, three type of electrodes based in LIG, silver chloride and carbon inks have been compared during the acquisition of bipotentials as electrocardiogram, electromyogram and electrooculogram. For this last one, a completely new framework for acquisition have been developed. This framework is based in a printed patch which integers 6 electrodes for the EOG acquisitions and an *ad-hoc* signal processing to detect the direction and amplitude of the eye movement. The performance of the developed electrodes have been compared with commercial ones using the characteristics parameters of each signal as comparative variables. The results obtained for the flexible electrodes have shown a similar performance than the commercial electrodes with an improvement in the comfort of the user.

INDEX TERMS Printed electronics, flexible electronics, electrodes, LIG, screen printing, ECG, EOG.

I. INTRODUCTION

Wearable devices (often simply referred to as ''wearables'') will play an important role in future paradigms in healthcare [1], [2], as part of the next generation of Internet of Things (IoT)-connected systems. These include the translation of the medical instrumentation to the patients' home, with the objective of continuous monitoring to prevent diseases such as cardiovascular conditions [3]. Several challenges arise when trying to achieve this objective, the biggest ones related to communications and acquisition of the biosignals. Regarding communications, security solutions are required since the transmitted data are personal information, while the optimization of IoT networks still remains an issue [4]–[7]. On the other hand, the ubiquitous acquisition of signals requires advanced signal processing and wearable devices with capabilities for long-term applications. Biopotential recordings such as Electrocardiogram (ECG), Electromyogram (EMG), Electroencephalogram (EEG) or Electrooculogram (EOG) are basic tools for health monitoring, as they provide valuable information on the health of the user in a non-invasive way. Thus, wearables to acquire this type of signals are key to improve medical systems and patient wellness [8], [9], and can be even used in innovative applications, such as attention monitoring [10].

Flexible electronics are a great tool to achieve the features described above. With these technologies, devices can be conformally adapted to the anatomy of the user without perturbing his/her activity. Thus, flexible electrodes are a key asset for this type of applications, especially for integration in a single device to be attached to the skin and that is able to communicate with healthcare personnel to remotely monitor patients. Traditionally electrical biosignals are acquired using Ag/AgCl wet electrodes. The behaviour

The associate editor coordinating the review of this manuscript and approving it for publication was Mohamad Forouzanfar.

of these wet electrodes is well-known and they have been widely studied in signal acquisition. However, they present several problems related to the comfort of the user, especially in cases of extremely sensitive skin and in long-term acquisition [11], [12]. Dry electrodes can mitigate these problems and it is in this field were flexible electronics are of great interest [13]. Moreover, flexible electronics open a wide field for innovative wearable devices [14]. New tools in the field of flexible electronics are currently available, such as printed electronics and, more recently, novel nanomaterials [15]–[17].

The most common technologies for printed electronics are screen and ink-jet printing. In the literature several examples of flexible electrodes using printing techniques on different substrates can be found. For example, Geng Yang *et al.* developed an ECG acquisition system over paper substrate using ink-jet printing [18]. Furthermore, Deberner *et al.* developed EEG electrodes printed over polyimide layers. Also, a system for the acquisition of multiple biosignals has been developed by Shustak *et al.*, integrating all the electrodes in a single adhesive patch [19]. Textiles have been also used as printing substrate by Lidón-Roger *et al.* [20] and Xu *et al.* [21].

More recently, graphene-based electronics have expanded the possibilities for flexible devices, since graphene is a biocompatible, conductive material [22]. For example, Celik *et al.* developed ECG electrodes based on chemical vapor deposition (CVD) over Ag/AgCl electrodes [23]. Additionally, Lou *et al.* [24] and Karim *et al.* [25] studied the application of graphene over textiles. Furthermore, Laser-Induced Porous Graphene (LIG) has been also used to create ECG electrodes [26], [27].

In this paper, these two technologies, screen printing and LIG applied to electrodes, are compared to traditional AgCl electrodes for the acquisition of ECG, EMG and EOG signals, since the behavior of this type of traditional electrodes is well-known and they are widely used in real applications. For screen-printing, carbon and silver pastes have been used. In the case of LIG electrodes, the substrate was Kapton, which allows for a cheaper fabrication process than CVD techniques. The electrodes are compared in the acquisition of ECG and EOG signals, using the influence of the electrode on the diagnostic characteristics of each signal as variable of comparison. It must be noted that EOG acquisition with this type of technologies is an innovative solution, demonstrated in this work with an *ad hoc* patch that can enable new possibilities in the use of this technology. As an example of this, measuring the EOG while an activity is carried out is achieved in a more ergonomic way than with traditional electrodes, while also interfering less with the user activity and requiring very simple digital signal processing. In contrast to CVD or stretchable LIG techniques, which require several steps to manufacture the electrode or complex materials as Polydimethylsiloxane (PDMS), the presented electrodes can be fabricated over low-cost materials in just one fabrication step. Furthermore, the required techniques here allow the design of any electrode layout as well as large-scale manufacturing.

The remaining of the paper is structured as follows: Section 2 provides details of the materials and methods used in this work. The results are then presented and discussed in Section 3. Finally, Section 4 summarizes the conclusions derived from this study.

II. MATERIALS AND METHODS

A. ELECTRODE DESIGN AND FABRICATION

The presented electrodes were designed with a circular form with a diameter of 10 mm and a small connector wire from the same material as the electrode. The techniques used are screen printing and LIG. In the market there are mainly 3 options for conductive pastes: silver, silver/silver chloride and carbon pastes. In this work, the EDAG 6038E SS E&C silver/silver chloride paste from Loctite (Henkel) [28] was selected, as it is specifically indicated for biosensors and its ratio of silver over silver chloride is 9:1, which results in a sheet resistance of 0.04 Ω/sq. The other selected paste was the carbon paste C-220 from Applied Ink Solutions [29], which is an thixotropic paste for screen printing with a sheet resistance around 16 Ω/sq. All pastes were deposited with a manual screen printer (Siebdruck Versand) using a screen mesh density of 120 threads/cm. Pastes were cured at 115 °C during 10 min. The electrodes are based in a multilayer structure as the one shown in Figure 1a. Electrode, wire and isolation layer have been printed over a polyethylene terephthalate (PET) substrate. Later, a stretchable adhesive skin patch and a back cover are added to adhere the electrode to the skin, which results in the electrodes shown in Figure 1b. To measure EOG, the electrodes have the same multilayer structure but with 6 electrodes integrated in a patch, as Figure 1c shows. This patch ensures the proper positioning of the electrodes and avoids cables interfering the user's vision. The designed electrodes have a sheet resistance of 0.062 Ω/cm^2 for silver and 23 Ω/cm^2 for carbon.

In the case of LIG electrodes, Kapton HN polyimide was used to obtain graphene-derived structures. This polyimide, which is produced from the condensation of pyromellitic dianhydride with 4,4-Oxydianiline as cross-linking agent, exhibits an excellent balance of physical, chemical and electrical properties over a wide temperature range. When the laser incises on the Kapton with enough energy to elevate its temperature, it produces a local ablation of the polyimide, thus achieving a conductivity comparable to that of graphene obtained by CVD [18]. Using this technique and the multilayer structure shown in Figure 2a, similar electrodes to the ones described above were created with a 2.4-W CO_2 laser. Later, a stretchable adhesive is added along with an AgCl contact for the connection wire, resulting in the electrode shown in Figure 2b. In Figure 2c, a SEM image of the electrode is shown, where the pattern generated by the CNC laser can be observed. The Raman spectrum is shown in Figure 2d, and it can be observed that it is composed of three peaks (D peak: 135 cm^{-1}; G peak: 158 cm^{-1}; 2D peak: 270 cm^{-1}) that confirm the graphene nature of the structure. However,

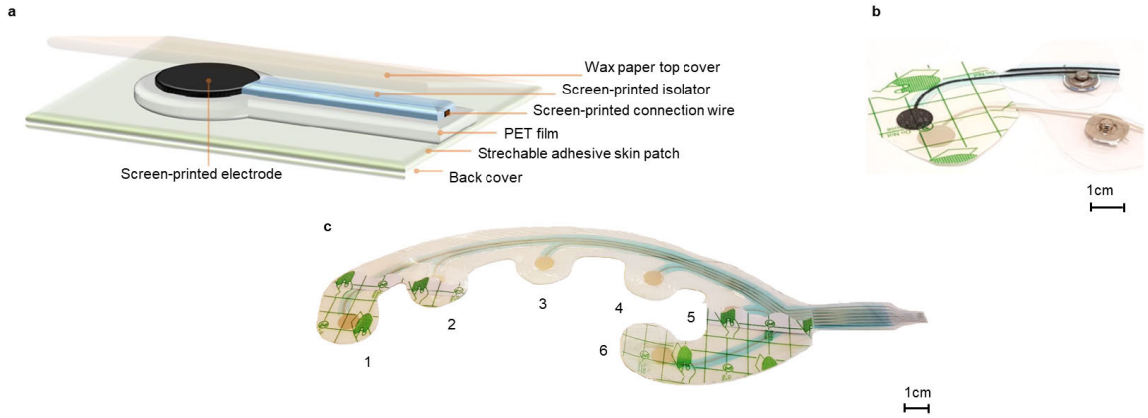

FIGURE 1. Screen printed electrodes. a multilayer structure used for each electrode. b Carbon (black) and silver (grey) electrodes for ECG. c Screen printed patch for EOG.

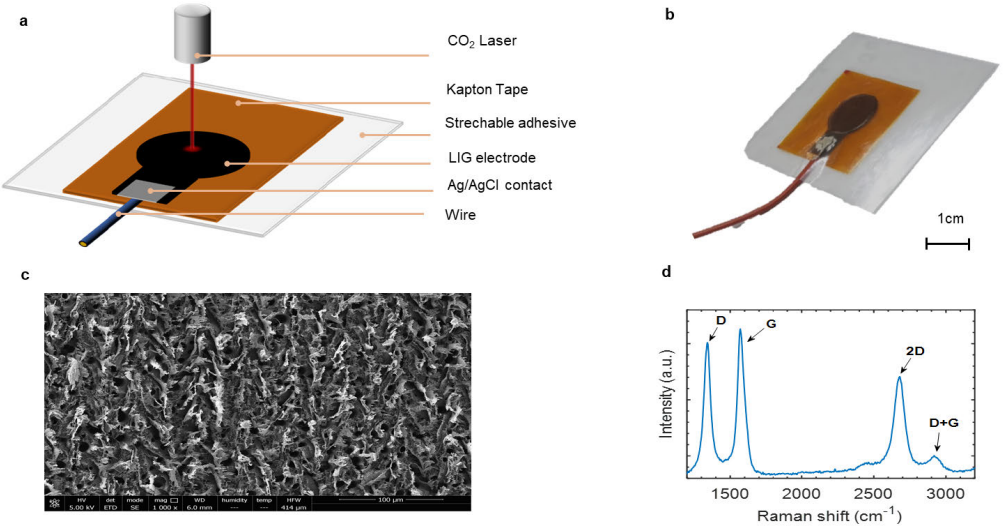

FIGURE 2. LIG electrodes. a multilayer structure of the electrode. b developed electrode. c SEM image. d Raman spectrum.

this structure differs from monolayer graphene, as the D and 2D peaks demonstrate. A I_D/I_G ratio close to 1 indicates the presence of defects in the crystalline structure of the graphene. The I_{2D}/I_G ratio confirms the multilayer structure of the graphene generated in the electrode [30]. The sheet resistance of the obtained electrode is 360 Ω/cm^2.

The described electrodes were compared to the commercial EL503 electrodes, manufactured by Biopac [31]. These electrodes are wet type electrodes with an Ag/AgCl contact and 11-mm diameter, along with a 35-mm adhesive patch and an sponge to confine the electrolyte.

In order to study the impedance of the electrodes, they were attached to a metallic plane to contact all the electrode surface. The impedance was thus measured with a Digilent Analog Discovery 2 impedance analyzer between the connection and the metallic plane. For the commercial electrode, electrolyte gel was also added to keep the same conditions than in real applications. In Figure 3, the results for all the electrodes are shown. Two main tendencies may be observed: LIG and commercial electrodes tend to have a capacitive behavior while screen printed electrodes have a purely resistive behavior. The one with lower impedance is the silver electrode while the highest is the impedance of the carbon one. Commercial and LIG electrodes have a similar impedance, around 700 Ω.

B. ECG ACQUISITION

To acquire signals, the sensing platform Biosignalsplux [32], created by PLUX wireless biosignals S.A., was used. This platform allows the acquisition of up to 8 channels of different type of signals. Several probes are available for this device to acquire a wide range of biosignals. In this work, the ECG probes were used to acquire both ECG and EOG signals. These probes have a differential input, with a third reference input. Their input range is ±1.5 V, with a gain of 1000 V/V and bandwidth from 0.5 Hz to 100 Hz.

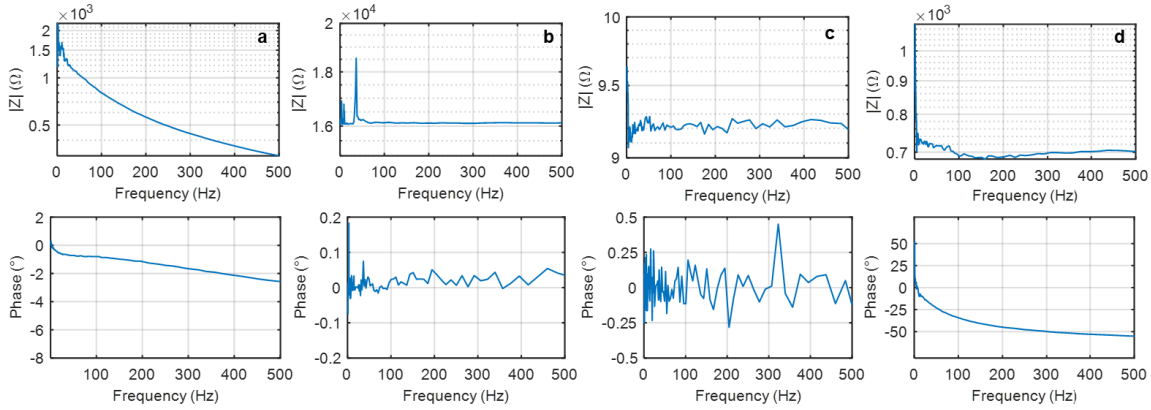

FIGURE 3. Impedance measurement for all the electrodes. a Module and phase of commercial electrodes, b Module and phase of carbon electrodes, c Module and phase for silver electrodes d Module and phase for LIG electrode.

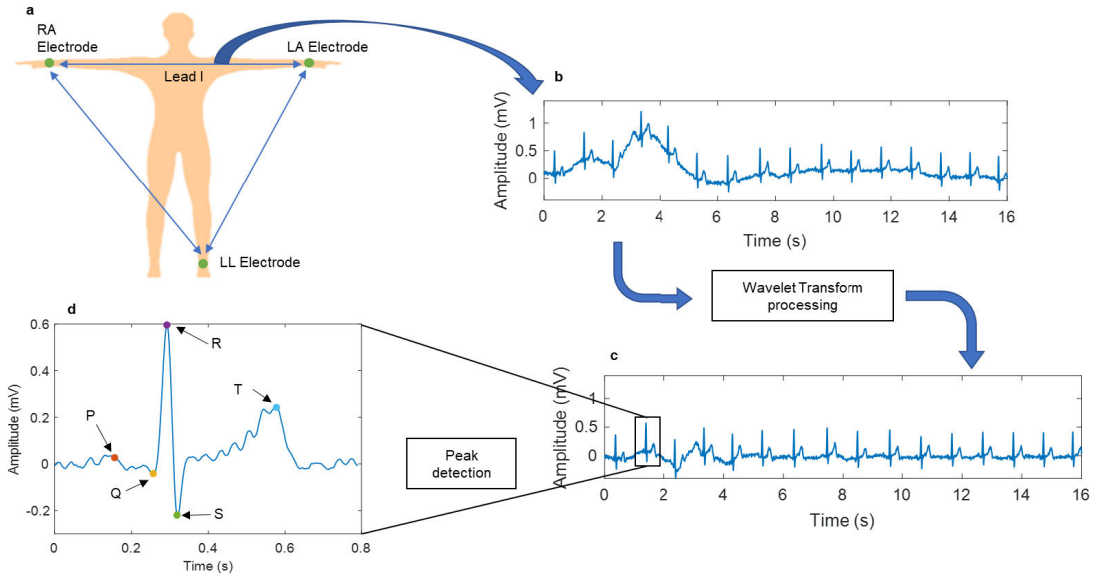

FIGURE 4. ECG acquisition and processing. a Position of the electrodes and leads. b Typical signal from Lead I. c Signal processed with wavelet Transform. d QRS complex detail.

ECG acquisition for all electrodes was carried out during 180 s using Lead 1, which requires to place an electrode on each wrist (the positive electrode is the one on the left arm, LA), and a third reference electrode on the ankle, as shown schematically in Figure 4a. All signals were consecutively acquired from two healthy test subjects using the different electrodes. Skin was cleansed with alcohol prior to electrode attachment, in order to remove any dirt or skin secretions that could affect the electrode contact. The electrodes were placed in the same positions in consecutive acquisitions. With this arrangement, the obtained typical ECG signal is shown in Figure 4b, where it is possible to observe a baseline deviation, usually refered to as wandering, as well as noise. To process the signal it is essential to suppress these artifacts. In this work, a processing based in the wavelet transform is used [33]. This processing obtains very low frequency and high frequency components through wavelet decomposition and later eliminates the bands where noise and wandering are contained. With this, the original signals are denoised, as illustrated in Figure 4c. Finally, signals are processed to detect the characteristic points shown in Figure 4d, which define the information related to the heart's behavior. The algorithm for this detection and annotation follows these steps, assuming a 1-ksps sampling rate:

1) Detect R-peaks finding maxima separated, at least, by 3000 samples
2) Find minima (Q-peaks) and maxima (P-peaks) 250 ms before the R-peaks
3) Find minima (S-peaks) and maxima (T-peaks) 500 ms after the R-peaks

C. EOG ACQUISITION

EOG acquisition was carried out with the same system and probes as in the case of ECG. However, in order to perform a more precise comparison, EOG requires an experimental setup that ensures the same amplitude and direction of the eye

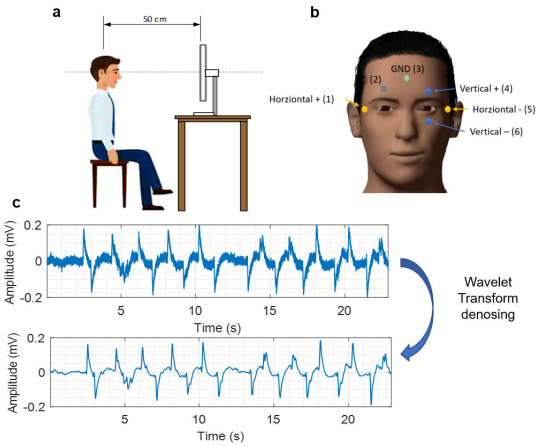

FIGURE 5. EOG acquisition method. a Position of the user during experiments. b Positions of the electrodes and signal nomenclature. c Wavelet denoising.

movement for all measurements. For this purpose, a specific measurement framework has been developed. First, a video (see supporting information) has been created as a guidance for the subject under study. The video consists of a red point describing a certain pattern in the screen, which the subject has to follow with his/her eyes during the experiment, completing the following sequence of movements:

1) Look right for 1 s, then look straight ahead for 1 s, repeat 5 times
2) Look left for 1 s, then look straight ahead for 1 s, repeat 5 times
3) Look up for 1 s, back to straight for 1 s, repeat 5 times
4) Look down for 1 s, back to straight for 1 s, repeat 5 times

Additionally to following the video pattern, it is also required that subjects are in the same position with respect to the screen in order to ensure the same movement. Subjects were thus positioned as shown in Figure 5a, at 50 cm from the screen and aligning their eyes to the centre of the screen. During the tests, winks can affect the subsequent processing of the signal. To avoid this interference, subjects under test were instructed to try to wink only in the intervals between movements, so the interference is easy to detect and can be avoided in the processing. If the user winked during movement, the test was repeated until it was ensured the absence of winks in the processing.

The patch shown in Figure 1c ensures the proper location of the electrodes, while two ECG probes, each one acquiring one of the axis of movement, were used. Despite the patch having six electrodes, only five of them were used to simplify the subsequent signal processing. The patch is designed to make the electrodes fall on adequate positions, with two electrodes (4 and 6) for vertical movements and other two (1 and 5) for horizontal movements, while the central electrode (3) is used as reference, as Figure 5b shows.

The EOG signals acquired following the same protocol as for ECG. Signals were thus consecutively acquired from two healthy test subjects using the different electrodes, while the skin was cleansed with alcohol to avoid differences in the skin state.

Finally, acquired data are processed using the wavelet transform. As shown in Figure 5c, the processing is applied only to suppress noise, as the wandering removal is not required and can even be detrimental in EOG signals. Thanks to the wavelet transform, almost all the noise is suppressed, thus facilitating the detection of movement direction.

D. EMG ACQUISITION

EMG signals were acquired with the EMG sensor of Biosignalsplux. This sensor has a differential input with a gain of 1000V/V and a bandwidth from 25 Hz to 500 Hz. The input range is the same as for the other sensor.

Muscles have two types of contractions: isotonic, in which the muscle varies its length, and isometric, in which the muscle does not vary its length. Despite EMG can be measured during both contractions, the isometric contraction is widely used for diagnosis of neurological diseases [34]. Concretely the typical procedure to study the EMG is through Maximum Voluntary Isometric Contraction (MVIC) [35]. In this work, EMG was measured in the biceps brachii at 100% of MVIC. To ensure the isometric contraction of the muscle, the test subject was required to position his elbow at 90° and push up against a fixed table.

The surface EMG measured in this work is a composition of all the evoked potential of the motor units of the muscle [34]. Due to this, the analysis of the signal is usually made by spectrum measurement, like Mean Frequency (MNF) and Median Frequency (MDF), which has been demonstrated to be useful in the study of muscle fatigue [36], [37]. Also, the recruitment of motor units of the muscle, during isometric contraction can be studied through MDF and MNF variations [38].

E. COMPARISON PARAMETERS

As detailed above, ECG, EMG and EOG signals were acquired, for comparison, with the developed electrodes as well as with the commercial ones. However, a proper numerical comparative must be carried out in order to provide an objective evaluation of the presented electrodes, so two variables have been used to compare the performance of the electrodes in each case.

For the ECG, QRS-complexes detected with the algorithm described above are compared to the annotations made by a cardiologist. The number of false positives (FP), false negatives (FN) and correctly or truly detected (TD) in the determination of QRS-complexes are used to compute the accuracy, A_{cc}, defined as [39]:

$$A_{cc} = \frac{TD}{TD + FN + FP} \tag{1}$$

When expressed as a percentage, 100% A_{cc} implies the detection of all the QRS-complexes without any false positives, while a 0% means no detection at all. This variable

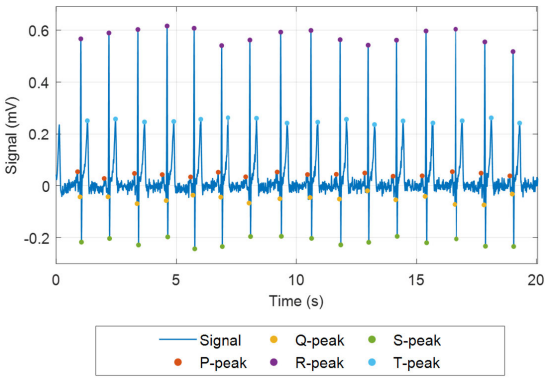

FIGURE 6. ECG signal acquired with the Ag/AgCl electrodes. QRST peaks noted by dots.

summarizes the SNR and distortion of the signals, since detection of QRS-complexes using each one of the characteristic points of the signal requires a clear and non-distorted waveform in order to achieve an adequate performance.

In the case of the EOG, the key variable is the direction of the movement. Thus, the comparison variable was the error in the determination of the movement direction. The relative error in the angle is one of the options to compare, but as the expected angles in each direction have different values, the error will be thus relative to different values. With the same absolute error, the relative error will be higher for lower angles, as 0 rad for example. To avoid this, the error is computed relative to a deviation of $\pm\frac{\pi}{4}$ from the expected angle:

$$\varepsilon = \frac{\theta_{expected} - \theta_{measured}}{\pi/4} \tag{2}$$

To be consistent with the ECG parameters, the accuracy of the EOG acquisition is defined as:

$$A_{cc} = 1 - \varepsilon \tag{3}$$

In this way, a correct determination of direction implies a 100% accuracy while a deviation of $\pi/4$ is represented by 0% accuracy.

For EMG the parameter that has been compared is MDF. Since in this case the real or expected value is unknown, the results from the commercial electrodes will be considered as the reference value. The relative error in MDF for the rest of the electrodes is thus computed as in Equation 4.

$$\varepsilon = \frac{MDF_{commercial} - MDF_{measured}}{MDF_{commercial}} \tag{4}$$

As with the EOG error and in order to be consistent with ECG values, the accuracy is defined as:

$$A_{cc} = 1 - \varepsilon \tag{5}$$

III. RESULTS AND DISCUSSION

The results obtained from the electrodes presented above and the results of the processing will be compared and discussed in this section. First, the ECG acquisition will be analyzed, later the EOG signals and finally EMG signals.

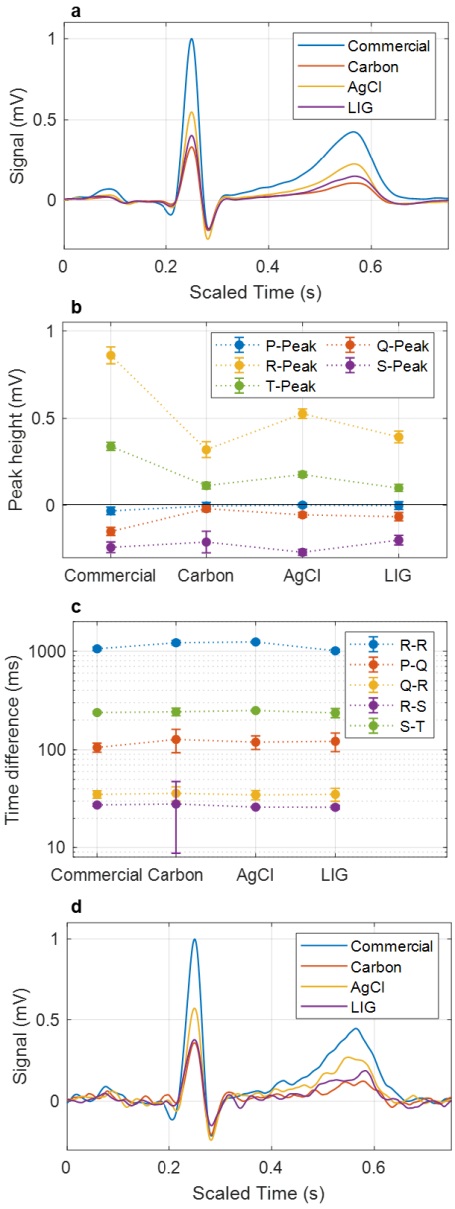

FIGURE 7. ECG comparative. a) Mean QRS-complex of each electrode. b) Amplitude comparison. c) Time segments comparison d QRS-complex comparative without averaging.

Although some limitations in the analysis exist, they equally affect all the tested electrodes. The first constrain is the acquisition in static position for both biosignals. This reduces the movement artifacts to low amplitude distortions associated with small movements. Anyway, such artifacts can be eliminated by wavelet processing [33]. These artifacts would increase its amplitude if the subject was moving. Due to this, a stretchable adhesive layer was used to improve adaptability to the skin through an improved skin contact. Furthermore, this contact could be achieved using stretchable substrates and stretchable pastes. However, this option

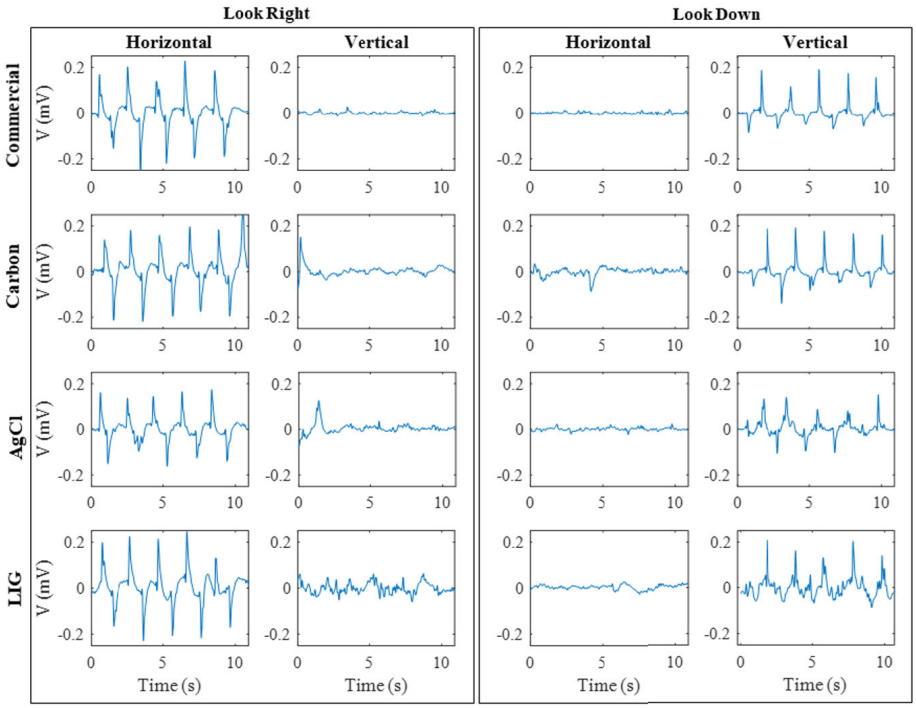

FIGURE 8. EOG signals for different materials and eye movements.

has not been considered due to the size of the electrodes. The second limitation is the lack of acquisition of the smooth pursuit movements in EOG, with only saccadic movement being acquired [40]. Nevertheless, saccadic movements are the most challenging for such electrodes as their frequency spectrum is wider.

A. ELECTROCARDIOGRAM

In Figure 6 a segment of an ECG signal acquired with the new Ag/AgCl electrode is shown. This signal has been processed with the techniques detailed above. It is also possible to observe the characteristic points detected by the algorithm.

Since a graphical comparative of the electrodes is quite difficult with a full 180 s recording, an average QRS has been obtained from the acquired signals. All the QRS-complexes from each recording have been aligned to the R-peak and averaged, resulting in the QRS-complexes shown in Figure 7a. The differences are thus quite clear, as the amplitudes are lower for the novel electrodes while the time durations of each peak are equal. The morphology of the signals is the same for all the electrodes but with lower amplitude. In Figure 7b and Figure 7c the mean amplitudes and mean time distance between peaks are shown, respectively, along with the standard deviation. As it can be seen, the amplitudes are reduced with the different electrodes, while the time segments are similar. It must be noted the variability of the R-S segment for carbon electrodes, due to noise and artifacts during acquisition. In Figure 7d, a comparison of a QRS complex without averaging is shown. It can be observed how the amplitudes are similar to the ones obtained with averaging. However, the noise can affect the lowest peaks (P and Q peaks). These results show that the electrodes with lower impedance have higher amplitude except for commercial electrodes, which can be due to a better contact thanks to electrode gel.

This comparison shows interesting results, but it does not cover some issues such as noise. In order to solve this, the accuracy in detection of QRS-complexes is shown in Table 1. The results confirm what it was expected from the graphical comparison, since the accuracy is reduced with the amplitude of the signals. In the case of carbon electrodes, the accuracy is lower when compared to the other alternatives, which is consistent with the higher variability in amplitudes and time segments previously observed. When compared to the commercial electrodes, a 3.13% reduction in accuracy is the worst case that has been observed.

B. ELECTROOCULOGRAM

An example of the signals obtained from the acquisition of EOG are shown in Figure 8, although for the sake of

TABLE 1. Accuracy for ECG acquisitions.

	FP	FN	TD	ACC
Commercial	0	0	840	100.00%
Carbon	18	5	712	96.87%
Ag/Cl	5	0	715	99.31%
LIG	8	0	877	99.10%

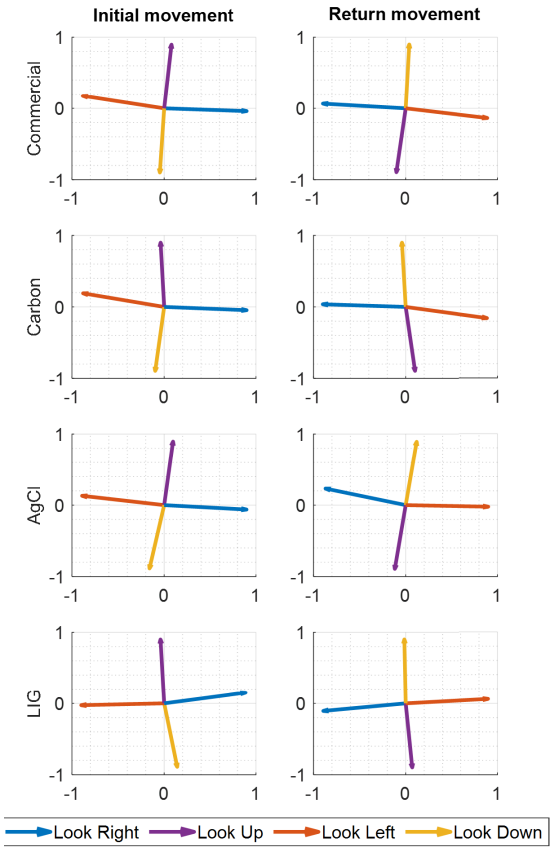

FIGURE 9. Vectors of movement obtained from the processing.

clarity only "look right" and "look down" movements are shown. Comparing the registers for each material, they are similar in terms of amplitude and pulse duration. As the frequency of these signals is so low and the position of the electrodes is so close to the origin of the signal, the impedance has lower influence. However, AgCl electrodes still shows slightly lower amplitude. In terms of noise, AgCl and LIG electrodes were observed to have worse SNR, despite the fact the wavelet transform was able to correct this lower SNR, as it is shown in Figure 8.

With the two channels acquired, detection of movement is a straight procedure, just composing both channels into a vector that determines the direction and amplitude of the movement. The determination is divided in two parts, first detect the movement in a given direction followed by the opposite direction and, second, detect the amplitude. As in each movement of the eye there will be two contiguous peaks, one for one direction and another one for the opposite, the detection first analyses the first peak sign and then determines the amplitude. The amplitude in this work is determined averaging the amplitude of the five peaks, according to the procedure described above, and normalizing it to their maximum amplitude. With this processing applied to each channel and combining both components in a vector it is possible to determine the direction as shown in Figure 9.

In Table 2 the accuracy of the results, obtained as detailed in the Methods section, is shown. The values are higher than 84% in all cases, and up to 87.87% in the best case for commercial electrodes. Among the developed electrodes, LIG electrodes are the closer to the results of the commercial alternative with 87.27% accuracy.

TABLE 2. Accuracy in the determination of movement direction from EOG acquisitions.

	Look right	Look left	Look down	Look up	Mean	θ
Commercial	94.44%	74.88%	93.38%	88.78%	**87.87%**	**9.00%**
Carbon	93.51%	72.81%	86.22%	94.50%	**86.76%**	**10.0%**
AgCl	91.24%	81.49%	77.39%	86.39%	**84.13%**	**6.00%**
LIG	78.45%	96.30%	79.97%	94.36%	**87.27%**	**9.36%**

It must be noted that, despite the error, the vectors of movement in one direction and its opposite should be parallel. Thus, any differences in the orientation of these vectors can be due to a non-perfect alignment of the electrodes' axis to the orientation of the cornea dipole. In this way, this difference in orientation can be used to correct the detected vectors by adding or subtracting this difference to the movement vectors. In Table 3 the relative parallelism error is shown. As it can be observed, the largest errors occur for the AgCl electrode with 6.1% "look right" movement. The rest of the movements and electrodes present lower errors, achieving a mean parallelism error of 2.04% $\pm$ 1.78%.

C. ELECTROMYOGRAM

Figure 10 shows the acquired EMG signals. While all the signals have an amplitude in the order of millivolts, commercial and LIG electrodes obtain higher amplitudes than screen printed electrodes. Commercial and LIG electrodes acquired an RMS value of 0.98 mV, while carbon electrodes resulted in an RMS value of 0.49mV and AgCl in 0.34 mV. In terms of noise, carbon and especially AgCl electrodes capture more noise than commercial and LIG electrodes. The spectrum of EMG signals extends over higher frequencies than the other signals studied so far, so the impedance has higher influence. As the results show, electrodes with capacitive behavior, as LIG and commercial ones, seem to have better performance while silver electrodes show lower amplitude.

As in the Methods section, EMG is typically analyzed through his spectrum, Figure 11 shows the power spectrum density (PSD) of the acquired EMG signals. Results show that there are no significant variances between them, but for the level of the signals that, as discussed above, is lower for AgCl and carbon electrodes. The information of the signal is focused below 100Hz and above 20Hz. In the cases of commercial and LIG electrodes, a local maximum around 150 Hz is observed, which can be explained as a 50 Hz noise harmonic.

Typical parameters that are analyzed in EMG diagnosis are Mean Frequency (MNF) and Median Frequency (MDF).

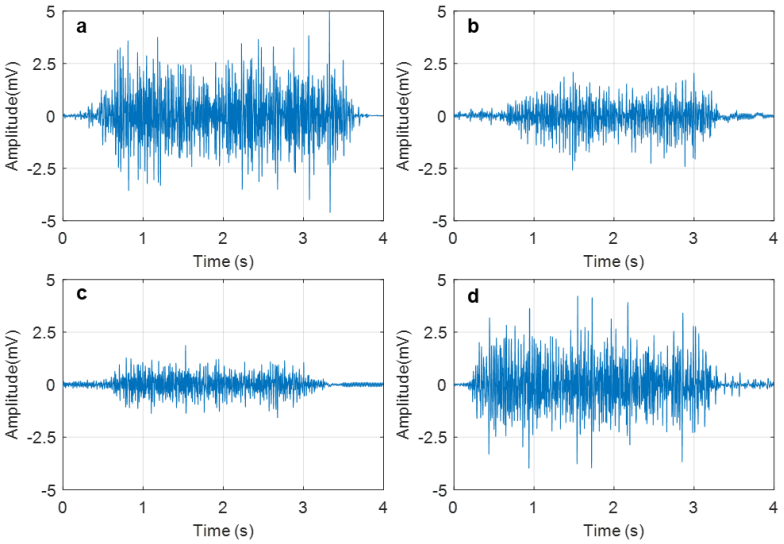

FIGURE 10. Raw EMG signals acquired a)Commercial, b)Carbon, c)AgCl, d)LIG.

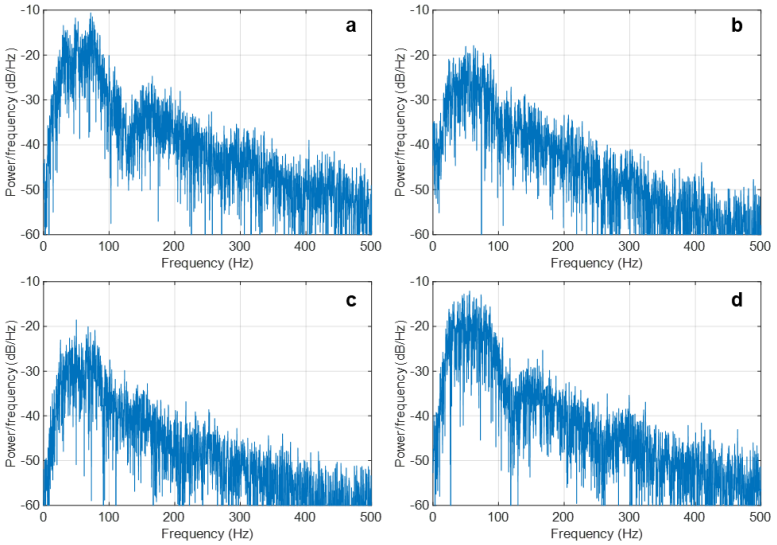

FIGURE 11. Power espectral density of the EMG signals acquired for each electrode a)Commercial, b)Carbon, c)AgCl, d)LIG.

TABLE 3. Parallelism error between initial and return movement of EOG.

	Look rigth	Look left	Look down	Look up	Mean	θ
Commercial	0.94%	1.44%	0.28%	0.77%	0.862%	0.478%
Carbon	0.30%	1.22%	4.87%	2.21%	2.16%	1.97%
AgCl	6.10%	3.85%	1.43%	0.77%	3.04%	2.43%
LIG	1.60%	1.30%	4.49%	1.08%	2.12%	1.59%

TABLE 4. EMG spectrum analysis results.

	MNF (Hz)	MDF (Hz)	RMS (mV)
Commercial	67.11	63.68	0.98
Carbon	69.20	61.67	0.49
AgCl	71.11	65.35	0.34
LIG	65.70	62.44	0.97

In Table 4 these parameters obtained from the acquired signals are shown. Mean frequency is around 70 Hz, with the LIG electrode showing more deviation from this value with a mean value of 65.70 Hz. Median frequencies are between 60 and 65 Hz. In this case, the AgCl electrodes is the one that differs from the others, but it is consistent with the mean values as it provides the higher mean value. In any case, as expected, all the electrodes provided similar frequencies without noticeable differences.

D. COST ANALYSIS

Regarding the cost of the electrodes, as the substrates are not expensive, the main cost is derived from the pastes, which is a big advantage for the LIG electrodes. These electrodes have a unit cost of 0.27€, while Ag/AgCl ones have a unit cost of 1.02€. The price of carbon electrodes is intermediate,

as the price of the carbon paste is lower than the silver paste's, keeping thus the unit cost at 0.56€. The unit cost of the commercial electrodes is around 0.50€, which is a similar price to carbon ones. Even if cost does not seem to be improved except for the LIG electrodes, it should be noted that the commercial electrodes are fabricated in mass, which results in much lower unit price when compared to the cost of the presented prototype electrodes. The electrodes developed in this work require techniques that can be easily moved to mass production, which will reduce their cost specially for screen printed electrodes.

Finally, Table 5 summarizes the main characteristics and results form each one of the presented electrodes.

TABLE 5. Summary of results obtained in this work.

	Commercial	Carbon	AgCl	LIG
Manufacturing complexity	High	Low	Low	Lowest
Sheet Resistance (Ω/cm^2)	0.255	23	0.062	360
ECG Accuracy	100 %	99.31 %	99.10 %	96.87 %
EOG Precision	87.87 %	86.76 %	84.13 %	87.27 %
EMG Accuracy	100 %	96.85%	97.38 %	98.05 %

IV. CONCLUSIONS

Three types of printed flexible electrodes have been presented in this work. Two technologies have been used, LIG over Kapton and screen printing with AgCl and carbon pastes. The electrodes have been compared acquiring ECG and EOG, showing a comparable performance to that of commercial electrodes, while they are much more comfortable for the user and their manufacturing costs are also lower.

In the case of ECG acquisition, all the tested systems were able to acquire ECG without distorting it, even if a reduction of the amplitude is observed. The accuracy obtained with these electrodes in ECG-point detection is higher than 96.9%, which is the worst case value obtained for carbon electrodes. The best-performing electrode has been the AgCl electrode, with 99.3% of accuracy. It should be noted that the commercial electrodes were wet type electrodes, while the developed electrodes are dry, which has some influence in their performance due to the skin-electrode contact resistance.

For EOG, the electrodes were integrated in an *ad hoc* adhesive patch, and a custom measurement procedure was developed. With this integration, not only the ability to track eye motion was shown but also ergonomics were improved thanks to this flexible electronics technology. In this test, all the electrodes acquired similar waveforms, with the only differences lying in the acquisition noise, which was in any case corrected with wavelet-based processing. Regarding the accuracy in direction detection, LIG electrodes showed the best performance with 87.3% accuracy, very close to commercial electrodes (87.9% accuracy). Parallelism between movements in opposite directions was also analysed. It must be noted too that the presented measurement procedure may help define new applications based on EOG acquisition, due to its simplicity and reproducibility.

Electrodes were also tested during the acquisition of surface EMG. All the electrodes were able to obtain EMG signals with different amplitudes but without noticeable differences in the obtained spectrums. Typical EMG parameters, MDF and MNF, were compared for all the electrodes obtaining similar values in all the cases with a maximum deviation lower than 5Hz.

Thus, it has been demonstrated that the electrodes developed in this work could be used in cost-effective wearable devices to monitor biomedical variables. In addition, the techniques used in this work provide several advantages regarding high volume production for the industry and user comfort, while maintaining an equivalent performance to that of conventional electrodes.

REFERENCES

[1] J. Andreu-Perez, D. R. Leff, H. M. D. Ip, and G.-Z. Yang, "From wearable sensors to smart implants—Toward pervasive and personalized healthcare," *IEEE Trans. Biomed. Eng.*, vol. 62, no. 12, pp. 2750–2762, Dec. 2015.

[2] P. J. Soh, G. A. E. Vandenbosch, M. Mercuri, and D. M. M.-P. Schreurs, "Wearable wireless health monitoring: Current developments, challenges, and future trends," *IEEE Microw. Mag.*, vol. 16, no. 4, pp. 55–70, May 2015.

[3] E. Wilkins, L. Wilson, K. Wickramasinghe, P. Bhatnagar, J. Leal, R. Luengo-Fernandez, R. Burns, M. Rayner, and N. Townsend, *European Cardiovascular Disease Statistics*. Brussels, Belgium: European Heart Network, Feb. 2017.

[4] X. Sun, S. Wang, Y. Xia, and W. Zheng, "Predictive-trend-aware composition of Web services with time-varying Quality-of-Service," *IEEE Access*, vol. 8, pp. 1910–1921, 2020.

[5] H. Zhang, H. Zhang, S. Pirbhulal, W. Wu, and V. H. C. D. Albuquerque, "Active balancing mechanism for imbalanced medical data in deep learning based classification models," *ACM Trans. Multimedia Comput., Commun. Appl.*, vol. 16, pp. 1–15, Mar. 2020.

[6] S. Pirbhulal, O. W. Samuel, W. Wu, A. K. Sangaiah, and G. Li, "A joint resource-aware and medical data security framework for wearable healthcare systems," *Future Gener. Comput. Syst.*, vol. 95, pp. 382–391, Jun. 2019.

[7] S. Pirbhulal, W. Wu, K. Muhammad, I. Mehmood, G. Li, and V. H. C. de Albuquerque, "Mobility enabled security for optimizing IoT based intelligent applications," *IEEE Netw.*, vol. 34, no. 2, pp. 72–77, Mar. 2020.

[8] A. K. Yetisen, J. L. Martinez-Hurtado, B. Ãœnal, A. Khademhosseini, and H. Butt, "Wearables in medicine," *Adv. Mater.*, vol. 30, Aug. 2018, Art. no. 1706910.

[9] D. Y. Kim, C.-H. Han, and C.-H. Im, "Development of an electrooculogram-based human-computer interface using involuntary eye movement by spatially rotating sound for communication of locked-in patients," *Sci. Rep.*, vol. 8, no. 1, p. 9505, Dec. 2018.

[10] J. Arnin, D. Anopas, M. Horapong, P. Triponyuwasi, T. Yamsa-ard, S. Iampetch, and Y. Wongsawat, "Wireless-based portable EEG-EOG monitoring for real time drowsiness detection," in *Proc. 35th Annu. Int. Conf. IEEE Eng. Med. Biol. Soc. (EMBC)*, Jul. 2013, pp. 4977–4980.

[11] R. J. Cochran and T. Rosen, "Contact dermatitis caused by ECG electrode paste," *Southern Med. J.*, vol. 73, no. 12, pp. 1667–1668, Dec. 1980.

[12] W. Uter and H. J. Schwanitz, "Contact dermatitis from propylene glycol in ECG electrode gel," *Contact Dermatitis*, vol. 34, no. 3, pp. 230–231, Mar. 1996.

[13] S. L. Kappel, M. L. Rank, H. O. Toft, M. Andersen, and P. Kidmose, "Dry-contact electrode ear-EEG," *IEEE Trans. Biomed. Eng.*, vol. 66, no. 1, pp. 150–158, Jan. 2019.

[14] Y. M. Chi, T.-P. Jung, and G. Cauwenberghs, "Dry-contact and noncontact biopotential electrodes: Methodological review," *IEEE Rev. Biomed. Eng.*, vol. 3, pp. 106–119, 2010.

[15] Z. Cui, *Printed Electronics: Materials, Technologies and Applications*. Singapore: Wiley, 2016.
[16] S. Yao and Y. Zhu, "Nanomaterial-enabled dry electrodes for electrophysiological sensing: A review," *JOM*, vol. 68, no. 4, pp. 1145–1155, Apr. 2016.
[17] F. Romero, A. Salinas-Castillo, A. Rivadeneyra, A. Albrecht, A. Godoy, D. Morales, and N. Rodriguez, "In-depth study of laser diode ablation of kapton polyimide for flexible conductive substrates," *Nanomaterials*, vol. 8, no. 7, p. 517, Jul. 2018.
[18] G. Yang, L. Xie, M. Mantysalo, J. Chen, H. Tenhunen, and L.-R. Zheng, "Bio-patch design and implementation based on a low-power System-on-Chip and paper-based inkjet printing technology," *IEEE Trans. Inf. Technol. Biomed.*, vol. 16, no. 6, pp. 1043–1050, Nov. 2012.
[19] S. Shustak, L. Inzelberg, S. Steinberg, D. Rand, M. D. Pur, I. Hillel, S. Katzav, F. Fahoum, M. De Vos, A. Mirelman, and Y. Hanein, "Home monitoring of sleep with a temporary-tattoo EEG, EOG and EMG electrode array: A feasibility study," *J. Neural Eng.*, vol. 16, no. 2, Apr. 2019, Art. no. 026024.
[20] J. Lidón-Roger, G. Prats-Boluda, Y. Ye-Lin, J. Garcia-Casado, and E. Garcia-Breijo, "Textile concentric ring electrodes for ECG recording based on screen-printing technology," *Sensors*, vol. 18, no. 1, p. 300, Jan. 2018.
[21] X. Xu, M. Luo, P. He, X. Guo, and J. Yang, "Screen printed graphene electrodes on textile for wearable electrocardiogram monitoring," *Appl. Phys. A, Solids Surf.*, vol. 125, no. 10, p. 714, Oct. 2019.
[22] R. You, Y. Liu, Y. Hao, D. Han, Y. Zhang, and Z. You, "Laser fabrication of graphene–based flexible electronics," *Adv. Mater.*, vol. 32, Aug. 2019, Art. no. 1901981.
[23] N. Celik, N. Manivannan, A. Strudwick, and W. Balachandran, "Graphene-enabled electrodes for electrocardiogram monitoring," *Nanomaterials*, vol. 6, no. 9, p. 156, Aug. 2016.
[24] C. Lou, R. Li, Z. Li, T. Liang, Z. Wei, M. Run, X. Yan, and X. Liu, "Flexible graphene electrodes for prolonged dynamic ECG monitoring," *Sensors*, vol. 16, no. 11, p. 1833, Nov. 2016.
[25] N. Karim, S. Afroj, A. Malandraki, S. Butterworth, C. Beach, M. Rigout, K. S. Novoselov, A. J. Casson, and S. G. Yeates, "All inkjet-printed graphene-based conductive patterns for wearable e-textile applications," *J. Mater. Chem. C*, vol. 5, no. 44, pp. 11640–11648, 2017.
[26] B. Sun, R. N. McCay, S. Goswami, Y. Xu, C. Zhang, Y. Ling, J. Lin, and Z. Yan, "Gas-permeable, multifunctional on-skin electronics based on laser-induced porous graphene and sugar-templated elastomer sponges," *Adv. Mater.*, vol. 30, no. 50, Dec. 2018, Art. no. 1804327.
[27] F. J. Romero, E. Castillo, A. Rivadeneyra, A. Toral-Lopez, M. Becherer, F. G. Ruiz, N. Rodriguez, and D. P. Morales, "Inexpensive and flexible nanographene-based electrodes for ubiquitous electrocardiogram monitoring," *NPJ Flexible Electron.*, vol. 3, no. 1, p. 12, Dec. 2019.
[28] *Inks and Coatingsprinted Electronics*, Henkel, Düsseldorf, Germany, 2017.
[29] *Technical Data Sheetc-220 Carbon Resistiveink*, A. I. Solutions, New Delhi, India, 2018.
[30] Y. Hao, Y. Wang, L. Wang, Z. Ni, Z. Wang, R. Wang, C. K. Koo, Z. Shen, and J. T. L. Thong, "Probing layer number and stacking order of few-layer graphene by Raman spectroscopy," *Small*, vol. 6, no. 2, pp. 195–200, Jan. 2010.
[31] *El500 Series—Disposable Electrodes*. BIOPAC Systems, Goleta, CA, USA, 2018.
[32] *Biosignal Acquisition Tool-Kit for Advancedresearch Applicationsuser Manual*. PLUX Wireless Biosignals S.A, Lisbon, Portugal, 2018.
[33] E. Castillo, D. P. Morales, A. García, F. Martínez-Martí, L. Parrilla, and A. J. Palma, "Noise suppression in ECG signals through efficient one-step wavelet processing techniques," *J. Appl. Math.*, vol. 2013, pp. 1–13, Jan. 2013.
[34] D. Farina, R. Merletti, and R. M. Enoka, "The extraction of neural strategies from the surface EMG," *J. Appl. Physiol.*, vol. 96, no. 4, pp. 1486–1495, Apr. 2004.
[35] D. Meldrum, E. Cahalane, R. Conroy, D. Fitzgerald, and O. Hardiman, "Maximum voluntary isometric contraction: Reference values and clinical application," *Amyotrophic Lateral Sclerosis*, vol. 8, no. 1, pp. 47–55, Jan. 2007.
[36] A. N. Pujari, R. D. Neilson, and M. Cardinale, "Fatiguing effects of indirect vibration stimulation in upper limb muscles- pre, post and during isometric contractions superimposed on upper limb vibration," *Roy. Soc. Open Sci.*, vol. 6, no. 10, Sep. 2018, Art. no. 190019.
[37] L. Qi, J. M. Wakeling, A. Green, K. Lambrecht, and M. Ferguson-Pell, "Spectral properties of electromyographic and mechanomyographic signals during isometric ramp and step contractions in biceps brachii," *J. Electromyogr. Kinesiol.*, vol. 21, no. 1, pp. 128–135, Feb. 2011.
[38] D. Farina, M. Fosci, and R. Merletti, "Motor unit recruitment strategies investigated by surface EMG variables," *J. Appl. Physiol.*, vol. 92, no. 1, pp. 235–247, Jan. 2002.
[39] E. Castillo, D. P. Morales, A. García, L. Parrilla, V. U. Ruiz, and J. A. Álvarez-Bermejo, "A clustering-based method for single-channel fetal heart rate monitoring," *PLoS ONE*, vol. 13, no. 6, Jun. 2018, Art. no. e0199308.
[40] D. Purves, G. J. Angustine, D. Fitzpatrick, L. C. Katz, A.-S. LaMantia, J. O. McNamara, and S. M. Williams, eds., *Neuroscience*. Sunderland, MA, USA: Sinauer Associates, 2001.

VÍCTOR TORAL received the B.Eng. degree in electronic engineering from the University of Granada, in 2017, and the M.Eng. degree in electronics engineering from the Polytechnic University of Madrid, in 2018. He is currently pursuing the Ph.D. degree with the Department of Electronics and Computer Technology, University of Granada. His current research interests include biomedical electronics, reconfigurable instrumentation, and flexible electronics.

ENCARNACIÓN CASTILLO received the M.Sc. and Ph.D. degrees in electronic engineering from the University of Granada, Granada, Spain, in 2002 and 2008, respectively. From 2003 to 2005, she was a Research Fellow with the Department of Electronics and Computer Technology, University of Granada, where she is currently an Associate Professor. During her research fellowship, she carried out part of her research with the Department of Electrical and Computer Engineering, Florida State University, Tallahassee, FL, USA. She has authored over 50 technical papers in international journals and conferences. Her current research interests include the protection of IP protection of very large-scale integration (VLSI) and field-programmable gate arrays-based systems, as well as residue number system arithmetic, VLSI and FPL signal processing systems, and the combination of digital and analog programmable technologies for smart instrumentation for biosignal processing. She also serves regularly as a reviewer for IEEE journals.

ANDREAS ALBRETCH received the master's degree in electrical engineering and information technology and the Ph.D. degree in printed electronics and printed sensors for the Internet of Things from the Technical University of Munich, in 2014 and 2018, respectively. He is currently with Cicor Technologies in the industrialization of aerosol jet printed electronics for mass and niches markets.

FRANCISCO J. ROMERO received the B.Eng. and M.Eng. degrees in telecommunication engineering, both with valedictorian mention, from the University of Granada, Spain, in 2016 and 2018, respectively. In 2015, he joined the Department of Electronics and Computer Technology, University of Granada, as an Undergraduate Researcher, and in 2017, he became a Ph.D. Student with the National Predoctoral Scholarship. His current research interests include graphene-based sensors, flexible electronics, and the IoT embedded systems.

ANTONIO GARCÍA (Senior Member, IEEE) received the M.A.Sc. degree in electronic engineering, the M.Sc. degree in physics (majoring in electronics), and the Ph.D. degree in electronic engineering from the University of Granada, Granada, Spain, in 1995, 1997, and 1999, respectively.

He was an Associate Professor with the Department of Computer Engineering, Universidad Autónoma de Madrid, Madrid, Spain, before joining the Department of Electronics and Computer Technology, University of Granada, where he actually serves as a Full Professor. He was also a Visiting Professor with the Department of Electrical and Computer Engineering, FAMU-FSU College of Engineering, Tallahassee, FL, from August 2017 to January 2018. He has authored more than 130 technical papers in international journals and conferences.

Dr. García is a CAS and SP Society Member. He received the National Award to the Best Academic Record for his M.A.Sc. degree. He serves as reviewer and a guest editor for several journals and has been part of the program committee for several international conferences on programmable logic.

NOEL RODRÍGUEZ received the Electronics Engineer degree (B.Sc. and M.Eng.) from the University of Granada, in 2004, obtaining the First National Award of University Education, and the double Ph.D. degree from the University of Granada and the National Polytechnic Institute of Grenoble, France, in 2008, with the Extraordinary Award.

He is currently a Tenured Professor of electronics with the Department of Electronics and Computer Technology and the Co-Founder of the Pervasive Electronics Advanced Research Laboratory (PEARL), University of Granada. He has coauthored 15 international patents and more than 100 scientific contributions. His current research interests include low-power energy conversion, electric mobility, new materials for electronic applications, and memristors.

PAOLO LUGLI (Fellow, IEEE) received the degree in physics from the University of Modena and Reggio Emilia, Italy, in 1979, and the M.Sc. and Ph.D. degrees in electrical engineering from Colorado State University, Fort Collins, CO, USA, in 1982 and 1985, respectively. He is currently the President of the Free University of Bozen-Bolzano. He has authored more than 350 scientific articles.

DIEGO P. MORALES received the M.Sc. degree in electronic engineering and the Ph.D. degree in electronic engineering from the University of Granada, Spain, in 2001 and 2011, respectively. He was an Associate Professor with the Department of Computer Architecture and Electronics, University of Almería, Spain. He joined the Department of Electronics and Computer Technology, University of Granada, where he currently serves as a Tenured Professor. His current research interest includes developing reconfigurable application.

ALMUDENA RIVADENEYRA received the master's degrees in telecommunication engineering, environmental sciences, and electronics engineering, and the Ph.D. degree in design and development of environmental sensors from the University of Granada, Spain, in 2009, 2009, 2012, and 2014, respectively. Since 2015, she has been with the Institute for Nanoelectronics, Technical University of Munich, where her work is centered in printed and flexible electronics with a special focus on sensors and RFID technology.